0026-895X/09/7604-903–917$20.00
MOLECULAR PHARMACOLOGY
Copyright © 2009 The American Society for Pharmacology and Experimental Therapeutics
Mol Pharmacol 76:903–917, 2009

Vol. 76, No. 4
56838/3517466
Printed in U.S.A.

Inhibition of Human Two-Pore Domain K^+ Channel TREK1 by Local Anesthetic Lidocaine: Negative Cooperativity and Half-of-Sites Saturation Kinetics[S]

Tapan K. Nayak, S. Harinath, S. Nama, K. Somasundaram, and S. K. Sikdar

Molecular Biophysics Unit (T.K.N., S.H., S.K.S.) and Department of Microbiology and Cell Biology (S.N., K.S.), Indian Institute of Science, Bangalore, Karnataka, India

Received April 5, 2009; accepted July 20, 2009

ABSTRACT

TWIK-related K^+ channel TREK1, a background leak K^+ channel, has been strongly implicated as the target of several general and local anesthetics. Here, using the whole-cell and single-channel patch-clamp technique, we investigated the effect of lidocaine, a local anesthetic, on the human (h)TREK1 channel heterologously expressed in human embryonic kidney 293 cells by an adenoviral-mediated expression system. Lidocaine, at clinical concentrations, produced reversible, concentration-dependent inhibition of hTREK1 current, with IC_{50} value of 180 μM, by reducing the single-channel open probability and stabilizing the closed state. We have identified a strategically placed unique aromatic couplet (Tyr352 and Phe355) in the vicinity of the protein kinase A phosphorylation site, Ser348, in the C-terminal domain (CTD) of hTREK1, that is critical for the action of lidocaine. Furthermore, the phosphorylation state of Ser348 was found to have a regulatory role in lidocaine-mediated inhibition of hTREK1. It is interesting that we observed strong intersubunit negative cooperativity (Hill coefficient = 0.49) and half-of-sites saturation binding stoichiometry (half-reaction order) for the binding of lidocaine to hTREK1. Studies with the heterodimer of wild-type (wt)-hTREK1 and Δ119 C-terminal deletion mutant ($hTREK1_{wt}$-Δ119) revealed that single CTD of hTREK1 was capable of mediating partial inhibition by lidocaine, but complete inhibition necessitates the cooperative interaction between both the CTDs upon binding of lidocaine. Based on our observations, we propose a model that explains the unique kinetics and provides a plausible paradigm for the inhibitory action of lidocaine on hTREK1.

The molecular mechanism of local anesthetic action on voltage-gated sodium (Na^+) channels and the resulting blockade of action potential propagation are well documented (Ragsdale et al., 1994). Besides the voltage-gated Na^+ channels, other ion channels and receptors have been implicated in the action of local anesthetics (Cuevas and Adams, 1994; Nishizawa et al., 2002). Increasing evidence suggests that local anesthetics potently block potassium current (Carmeliet et al., 1986), which potentiates local anesthetic-induced inhibition of action potential firing (Drachman and Strichartz, 1991). In heterologous and native preparations, several voltage-gated potassium channels, including human (h)$K_v1.5$, $K_v2.1$, K_vLQT, and G protein-coupled inward rectifying K^+ channels have been identified as targets of local anesthetics (González et al., 2001; Zhou et al., 2001; Kindler et al., 2003). Modulation of K^+ channel function, by local anesthetics, may influence the transmission of sensory impulses by altering the resting membrane potential, repolarization after an action potential, and firing frequency of a neuron (Komai and McDowell, 2001). These studies indicate that the effects of local anesthetics in neural tissue may extend beyond the known direct actions on voltage-gated sodium channels (Kindler and Yost, 2005).

A new superfamily of K^+ channels, the tandem pore domain K^+ (K_{2P}) channels, has been cloned and characterized (Honoré, 2007). It was found to contribute to background or leak K^+ conductances involved in maintaining the resting

This research was supported by the Department of Science and Technology, Government of India. T.K.N. was supported by the Senior Research fellowship from Council of Scientific and Industrial Research, India.

Article, publication date, and citation information can be found at http://molpharm.aspetjournals.org.

doi:10.1124/mol.109.056838.

[S] The online version of this article (available at http://molpharm.aspetjournals.org) contains supplemental material.

ABBREVIATIONS: h, human; K_{2P}, tandem pore domain K^+; TREK1, TWIK-related K^+; CTD, C-terminal domain; PKA, protein kinase A; HEK, human embryonic kidney; PCR, polymerase chain reaction; wt, wild type; Ad, adenovirus; GFP, green fluorescent protein; I-V, current-voltage; NP_o, product of the number of channels (*N*) in a patch and the probability that the channel would be in the open state, P_o; TCE, 2,2,2-trichloroethanol; QX314, 2-((2,6-dimethylphenyl)amino)-*N*,*N*,*N*-triethyl-2-oxoethanaminium; KT 5720, (9*S*,10*S*,12*R*)-2,3,9,10,11,12-hexahydro-10-hydroxy-9-methyl-1-oxo-9,12-epoxy-1*H*-diindolo[1,2,3-*fg*:3′,2′,1′-*kl*]pyrrolo[3,4-*i*][1,6]benzodiazocine-10-carboxylic acid hexyl ester; NTD, N-terminal domain; AA, arachidonic acid; C, closed state; O, open state.

membrane potential and firing pattern of excitable cells (Lesage et al., 1996). These channels are modulated by a wide array of cellular lipids and pharmacological agents, including polyunsaturated fatty acids, second messengers, and general anesthetics (Honoré, 2007). Most of the members of this family are expressed widely in the central and peripheral nervous system. Local anesthetics have been identified as potent inhibitors of the K_{2P} channels causing membrane depolarization, which in turn promotes switching of voltage-gated Na^+ channels to open and inactivation states, thereby increasing their affinity for local anesthetics. Moreover, increases in neuronal excitability due to inhibition of K_{2P} channels may contribute to the cardiotoxic and excitotoxic side effects of local anesthetics (Kindler et al., 2003). Bupivacaine, one of the most potent and toxic local anesthetics clinically used, inhibits the K_{2P} channels TWIK-related acid-sensitive K^+ channel 1 and TREK1 at clinically relevant concentrations achieved by intravascular injection (~20 μM) (Punke et al., 2003; Kindler and Yost, 2005). Lidocaine, an amide local anesthetic, was found to inhibit K_{2P} channel TWIK-related acid-sensitive K^+ channel 2 at clinical doses (Kindler et al., 2003). However, the effect of lidocaine on human TREK1, the most thoroughly studied K_{2P} channel, has not been investigated.

Lidocaine, traditionally used as a local anesthetic and an antiarrhythmic drug, also exerts several unwarranted effects such as neurotoxicity, bronchial hyper-responsiveness, ototoxicity (ringing paresthesia), and convulsions at higher concentration in various clinical settings (Benkwitz et al., 2003). In contrast, central nervous system excitation, leading to seizures, has been partly attributed to local anesthetic action on K_{2P} channels, especially TREK1 (Kindler and Yost, 2005). Lidocaine has also been known to have inhibitory effects on neurophysiologic responses evoked by Aδ and C fibers in the dorsal root ganglion (Ness, 2000). Human tissue distribution assays indicate a prominent expression of TREK1 in dorsal root ganglia and the spinal cord. Furthermore, TREK1 has also been strongly implicated in pain perception and can be activated by nociceptive stimuli, including pressure and heat (Honoré, 2007). The above-mentioned evidence suggests a possible interaction of lidocaine with the TREK1 channel, which might explain its clinical actions.

In the present work, we investigated the effect of lidocaine on human TREK1 channels. In a heterologous expression system, at the whole-cell as well as single-channel level, lidocaine produced rapid and reversible inhibition of hTREK1. Experiments with the deletion mutants revealed the importance of the distal 89 residues of the C-terminal domain (CTD) of hTREK1 in mediating the effect of lidocaine. Furthermore, from site-directed mutagenesis studies, we identified a subdomain in the CTD comprising an aromatic couplet, Tyr352 and Phe355, adjacent to the protein kinase A (PKA) phosphorylation site Ser348, which was critical for the inhibitory action of lidocaine. It is interesting that we also observed strong negative cooperativity and half-of-sites saturation kinetics for the interaction of lidocaine with the channel. Kinetic analysis of the heterodimer of wild-type hTREK1 and CTD deletion mutant provided insight into the unique kinetic mechanism of lidocaine binding to hTREK1.

In conclusion, our results suggest that lidocaine, at clinical concentrations, potently inhibits the hTREK1 channel by binding to a putative lidocaine binding site in the CTD of hTREK1. Furthermore, binding of lidocaine to the CTD of the two monomers of hTREK1 induces an intersubunit negative cooperativity at single-channel level.

Materials and Methods

Cell Culture and Molecular Biology Reagents. Human embryonic kidney (HEK) 293 cells were maintained in Dulbecco's modified Eagle's medium-Ham's F-12, supplemented with 10% fetal bovine serum (v/v), 1% antibiotic-antimycotic (Sigma-Aldrich, St. Louis, MO), and gentamicin (50 μg/ml) (Sigma-Aldrich) in a humidified incubator with 5% CO_2. cDNA encoding the hTREK1 channel (GenBank accession AF004711) cloned in the mammalian expression vector pRAT (kindly donated by Prof. Steve A. N. Goldstein, Yale University Medical School, New Haven, CT) was used for the construction of recombinant hTREK1 adenovirus. The AdEasy-1 adenoviral vector system, including the pAdTrack-cytomegalovirus (shuttle vector), pAdEasy-1, and the electrocompetent cells of BJ5183 strain of *Escherichia coli*, was a generous gift from Prof. Bert Vogelstein (John Hopkins Oncology Center, Baltimore, MD). The C-terminal deletion mutants of hTREK1 (Δ89 and Δ119 hTREK1) were constructed by PCR mutagenesis as described previously (Harinath and Sikdar, 2004), and the S348A mutant of hTREK1 was a generous gift from Prof. Steve A. N. Goldstein (Yale University Medical School). The other site-directed mutageneses such as the S348D, S366A, and Y352A/F355A were performed with a QuikChange kit (Stratagene, La Jolla, CA), and mutations were verified by DNA sequencing that is illustrated in Supplemental Fig. S4. The primers for the PCR mutagenesis are listed in the Supplemental Data. For electrical recordings from the mutants (deletion as well as substitution), HEK 293 cells were transiently transfected with the mutant hTREK1 cDNA using the calcium phosphate method. In brief, the complex of calcium and DNA (0.5 μg of cDNA of the mutant hTREK1 along with 0.33 μg of enhanced green fluorescent protein) was added to HEK 293 cells cultured in 35-mm dishes. After 4 h of incubation, the cells were replenished with fresh medium after a brief osmotic shock using 10% glycerol in phosphate-buffered saline. The cells were used for electrophysiological experiments after 24 to 30 h of transfection. Transfected cells were identified by the green fluorescence from cells expressing enhanced green fluorescent protein in a standard fluorescence microscope. For the study of the heterodimer, wt-hTREK1 and Δ119 mutant cDNA were cotransfected in HEK 293 cells in equimolar ratio by the calcium phosphate method (Czirják and Enyedi, 2002).

Construction of Recombinant hTREK1 Adenovirus and Gene Transfer. We used the efficient homologous recombination machinery of *E. coli* with the AdEasy-1 system for the construction of adenovirus as described previously (He et al., 1998). In brief, the SalI/XbaI restriction fragment from the pRAT-hTREK1 was cloned into the shuttle vector pAdTrack-cytomegalovirus at the corresponding sites. The resultant plasmid (pAdTrack-hTREK1) was linearized with PmeI and cotransformed with the adenoviral backbone vector pAdEasy-1 into the BJ5183 cells by electroporation. Homologous recombinants containing the hTREK1 cDNA were detected by restriction digestion and agarose gel electrophoresis. Recombinant hTREK1 adenovirus (pAd-hTREK1) was then transformed into *E. coli* DH10B cells for large-scale amplification. The PacI-digested pAd-hTREK1 was transfected into HEK 293 cells by the classic calcium phosphate method, and the hTREK1 adenovirus was expanded, purified, and titered as described previously (He et al., 1998). The recombinant adenovirus encoding green fluorescent protein (Ad-GFP) was used as control. The efficiency of packaging and amplification of adenovirus could be determined by GFP expression.

For adenoviral infection, subconfluent (80–90% confluence) HEK 293 cells were incubated with Ad-hTREK1 or Ad-GFP at a multiplicity of infection of 15 to 20 at 37°C in normal growth medium. After 2 h of incubation, the infection medium was replaced with fresh

medium, and the cells were further incubated for 20 to 30 h. Subsequently, the infected cells were used for quantitative real-time PCR or regular electrophysiological experiments. Most of the electrophysiology experiments were carried out in HEK 293 cells infected with Ad-hTREK1 unless otherwise mentioned.

Reverse Transcription-PCR and Quantitative Real-Time PCR. Total cell RNA was prepared from the infected HEK 293 cells by using the TRIzol reagent (Aldrich Chemical Co., Milwaukee, WI). First-strand cDNA was synthesized using the ProtoScript cDNA synthesis kit (New England Biolabs, Ipswich, MA) using the murine leukemia virus reverse transcriptase and random primers. The reverse transcription product was amplified with hTREK1 specific primers (forward, 5′-GCTGTCCTGAGCGGATCCGGAGATTGGCTCCG-3′ and reverse, 5′-GGTTTAGTGGTAGTCGACTTATTAATTTGATGTTCTCAATCAC-3′; Sigma-Aldrich) and specific primers for the human glyceraldehyde-3-phosphate dehydrogenase, which served as the positive control.

Quantitative real-time PCR was performed using SYBR Green chemistry in 96-well optical plates on an ABI prism 5700 sequence detector (Applied Biosystems, Foster City, CA). The standard curves were generated by the regression analysis of the mean values of three multiplex PCRs for the $\log_{10}$-diluted cDNA. Real-time PCR was run for hTREK1 and human β-actin using cDNA corresponding to 200 ng of total cell RNA and gene-specific primers (specified above) using the DyNamo master mix (New England Biolabs) as per the manufacturer's instructions. Before quantification of real-time data, the specificity of the amplified product was examined by agarose gel electrophoresis and by dissociation curve analysis. For comparison of gene expression levels, all quantification were normalized to endogenous β-actin levels to account for variability in the initial concentration and quality of total RNA in the conversion efficiency of the reverse transcriptase reaction. The standard-curve method was used for quantification and normalization of cDNA amplification.

Electrophysiology, Anesthetic Application, and Data Analysis. Electrophysiological recording was performed using an EPC8 patch-clamp amplifier (HEKA Elektronik, Lambrecht/Pfalz, Germany). Whole-cell current and membrane potential were measured with the voltage-clamp and current-clamp methods, respectively, of the patch-clamp technique. Borosilicate micropipettes of 2- to 5-MΩ resistance were used for whole-cell recordings. Single-channel current recordings were acquired in the excised inside-out configuration of patch-clamp using fire polished micropipettes of 5- to 10-MΩ resistance, whose tips were coated with Sylgard (General Electric, Waterford, NY) to reduce capacitive noise (Hamill et al., 1981). The recordings were filtered at 3 KHz using a seven-pole Bessel filter (~3 dB), digitized using an LIH 1600 A/D converter interface (HEKA Electronik) at a sampling rate of 20 kHz and analyzed offline by Pulse (HEKA Electronik) and TAC software (Bruxton Corp., Seattle, WA). In experiments using the excised patches, pipette and bath solutions contained 155 mM KCl, 5 mM EGTA, 3 mM $MgCl_2$, and 10 mM HEPES (pH adjusted to 7.4 with KOH). In whole-cell recordings, bath solution contained 145 mM NaCl, 2.5 mM KCl, 3 mM $MgCl_2$, 1 mM $CaCl_2$, and 10 mM HEPES (pH adjusted to 7.4 with NaOH), whereas the pipette was filled with the intracellular solution containing 150 mM KCl, 3 mM $MgCl_2$, 5 mM EGTA, and 10 mM HEPES (pH adjusted to 7.4 with KOH). All recordings were done at room temperature and by holding the cell at −80 mV.

Whole-cell hTREK1 current was elicited by either a voltage ramp (300 ms) or incrementing voltage steps (50 ms) from −100 to 60 mV (interpulse interval, 5 s) unless specified. The time-dependent component was obtained from the activation time course of the whole-cell current by fitting it with a monoexponential function of the form $y = y_0 + a[1 - \exp(-x/\tau)]$. In contrast, the inhibition time course was fitted with one or two decaying exponential functions of the form $y = y_0 + a \times \exp(-x/\tau)$ to obtain the decay time constant for lidocaine-mediated inhibition. Single-channel current recording was acquired in gap free mode from a holding pipette potential of 0 mV. Single-channel events were detected by setting a threshold at half the maximal open channel current amplitude of the major conductance state (Colquhoun and Sigworth, 1983). Single-channel current amplitude was determined by constructing amplitude histograms and fitting with Gaussian distributions. Unitary current amplitudes obtained at different membrane potentials were used to plot the current-voltage (I-V) relationship. hTREK1 channel activity in a patch was expressed quantitatively as the NP_o [i.e., the product of the number of channels (N) in a patch and the probability that the channel would be in the open state, P_o]. The NP_o was calculated by the relative area under all points amplitude histogram and expressed as follows: $NP_o = \Sigma_{i=1}^{N} i \cdot A_i / \Sigma_{i=0}^{N} A_i$, where A is the area under the Gaussian curve and i is the number of active channels in a given recording fragment. For the NP_o analysis, it was assumed that the channels in a patch are identical and independent. The relative change in NP_o was obtained by measuring the average NP_o from approximately 1- to 2-min recordings. Dwell time distribution histograms were obtained by plotting the number of events against appropriately binned time interval. While constructing the dwell time histograms, the missed events were appropriately taken into account (Colquhoun and Sigworth, 1983). A maximum likelihood method was used to fit the histograms with a sum of exponential probability density functions to yield the mean dwell times or the time constants (τ_o, τ_c) (Colquhoun and Sigworth, 1983).

Stock solutions of the local anesthetic lidocaine (10 mM; Sigma-Aldrich), 2,2,2-trichloroethanol (TCE, 10 mM; Aldrich Chemical), and QX314 (10 mM) (lidocaine *N*-ethyl bromide; kindly provided by Dr. Rune Sandberg (Astra Pain Control, Sodertalje, Sweden) were freshly prepared in the extracellular saline solution. The stock solutions of forskolin (10 mM; Sigma-Aldrich), the PKA activator, and KT 5720 (5 mM; Alomone Labs, Jerusalem, Israel), the PKA inhibitor, were prepared in dimethyl sulfoxide. Test solutions of the drugs were prepared by diluting the stock solution in the extracellular solution. The final concentration of dimethyl sulfoxide was less than 0.1% in the test solutions, which was found to have no effect on the channel. The anesthetic and the drug solutions were applied locally to the cells or very close to the patch by either pressure ejection (PLI-100; Medical Systems Corp., Greenvale, NY) or by a hydrostatic pressure-driven fast perfusion device controlled by six-channel valve controller (VC-6; Warner Instruments, Hamden, CT). During application of the anesthetic, the bath was continuously perfused with the extracellular solution. For dose-response experiments, NP_o of hTREK1 channel was measured at −60 mV in the presence and absence of the drug over a period of 2 min. The percentage of change in the NP_o by a drug was quantified at various test concentrations according to the following equation: % change = $100\ [(NP_{oDrug} - NP_{oControl})/NP_{oControl}]$, where NP_{oDrug} and $NP_{oControl}$ were the measured NP_o after and before application of the drug, respectively. Steady-state concentration response of hTREK1 was fitted to the Hill equation of the form $y = (a \cdot x^b)/(c^b + x^b)$, where y is hTREK1 response, x is drug concentration, a is maximal response, b is the Hill coefficient, and c is half-maximal inhibitory or activating concentration. Single-channel currents, in presence of the anesthetic, were recorded only in the steady state. All results have been presented as the mean ± S.E.M. Results were considered significant when $p < 0.05$ in the Student's t test or nonparametric test such as the Mann-Whitney U test.

Results

Expression of hTREK1 in HEK 293 Cells. HEK 293 cells infected with Ad-hTREK1 exhibited a high level of hTREK1 mRNA expression, whereas the uninfected and control adenovirus (Ad-GFP)-treated cells failed to induce the expression of hTREK1. Figure 1, a and b, shows the SYBR Green real-time PCR kinetic data traces of hTREK1 and the corresponding dissociation curves, respectively. A melting temperature higher than 75°C indicates no primer-dimer formation (Fig. 1b), whereas a single band of desired size in

agarose gel electrophoresis (~0.4 kilobase) confirms the specificity of amplification of hTREK1 in the real-time PCR reaction (Fig. 1c). Figure 1d illustrates the -fold increase in the expression of hTREK1 in the Ad-hTREK1-infected cells. The expression of the hTREK1 mRNA was accompanied by enhanced whole-cell hTREK1 channel current, which was assayed by patch-clamp experiments.

Lidocaine Inhibits Whole-Cell hTREK1 Current. hTREK1, when expressed in infected HEK 293 cells, formed functional channels with kinetics similar to that described previously (Harinath and Sikdar, 2004). In physiological K^+ gradient, an outwardly rectifying, noninactivating, time-dependent current progressively developed upon depolarization, which was absent in uninfected cells and Ad-GFP-infected cells (Supplemental Fig. S1, a and b). We evaluated the sensitivity of hTREK1 to varying concentrations of the local anesthetic lidocaine (10 μM–5 mM). The reported plasma concentration of lidocaine is estimated between 20 and 30 μM when lidocaine is administered intravenously for arrhythmia or neuroprotection (Johnson et al., 2004), whereas local anesthetic-induced seizure and cardiovascular collapse ensue when the plasma concentrations of lidocaine exceeds 50 μM (DeToledo, 2000). During spinal or epidural anesthesia, lidocaine concentration in the cerebrospinal fluid normally reaches as high as 10 mM for the first 15 min after injection (Johnson et al., 2004). Thus, the steady-state concentration of lidocaine in the central nervous system and peripheral nervous system in various clinical conditions commensurate with the range we have used in the current study. In this physiological concentration range, lidocaine was found to inhibit the whole-cell hTREK1 current in a dose-dependent manner. Figure 2a illustrates hTREK1 current elicited by ramp changes in membrane potential (−100 to 100 mV) on application of increasing concentrations of lidocaine. The current inhibited by lidocaine reversed close to −90 mV (Fig. 2a), as predicted by the Nernst equation for a purely K^+-selective channel. On washing out, the inhibitory effect of the anesthetic could be reversed (Fig. 2b). The inhibition of hTREK1 current upon application of varying concentrations of lidocaine was described by the Hill equation (see *Materials and Methods*). The half-maximal inhibitory concentration (IC_{50}) and the Hill coefficient (α_H) were estimated to be 207 ± 31 μM and 0.49 ± 0.08, respectively (Fig. 2c). A Hill coefficient less than 1 indicates negative cooperativity in the interaction of lidocaine with the hTREK1 channel.

Inhibition of hTREK1 channel current was expected to result in membrane depolarization. Consistent with this hypothesis, lidocaine caused an immediate and reversible depolarization of the membrane of cells expressing hTREK1 channels (Fig. 2d). At a concentration of 0.5 mM, lidocaine caused membrane depolarization by 14.7 ± 1.2 mV ($n = 5$). The hTREK1 current has two distinct components: 1) an instantaneous component and 2) a time- and voltage-dependent component. The time-dependent component was quantified by fitting the activation time course with monoexponential function (see *Materials and Methods*; Fig. 2e). Lidocaine, at all test concentrations, caused significant inhibition ($p < 0.01$, Mann-Whitney U test; $n = 7$) of both the time-dependent and non–time-dependent components of hTREK1 current (77.8 ± 7.3 and 57.6 ± 11.4%, respectively, in the presence of 1 mM lidocaine, $n = 7$) (Fig. 2f) compared with the control (0 mM lidocaine). Voltage dependence of inhibition was analyzed by quantifying the reduction in whole-cell current amplitude at three different membrane potentials: −40, 0, and 40 mV at a concentration of 0.1 mM lidocaine (Fig. 2g). Inhibition of hTREK1 channels, however, was voltage-independent (43.7 ± 3.6, 40.7 ± 1.5, and 40.5 ± 1.3% at −40, 0, and 40 mV, respectively; $p > 0.05$, Mann-Whitney U test; $n = 4$) (Fig. 2g).

Inhibition of Single hTREK1 Channel by Lidocaine. The inhibitory effect of lidocaine was observed in excised inside-out patches containing single hTREK1 channels. Figure 3a, i, shows the representative single hTREK1 channel current traces evoked at different membrane potentials in symmetrical K^+ gradient in presence of 3 mM Mg^{2+} in the bath. The single-channel current reversed at 0 mV and exhibited mild outward rectification (Fig. 3, a and b), which is characteristic of the hTREK1 channel. The single-channel I-V relationships of hTREK1 in physiological and symmetrical gradients of K^+ were plotted by measuring the unitary

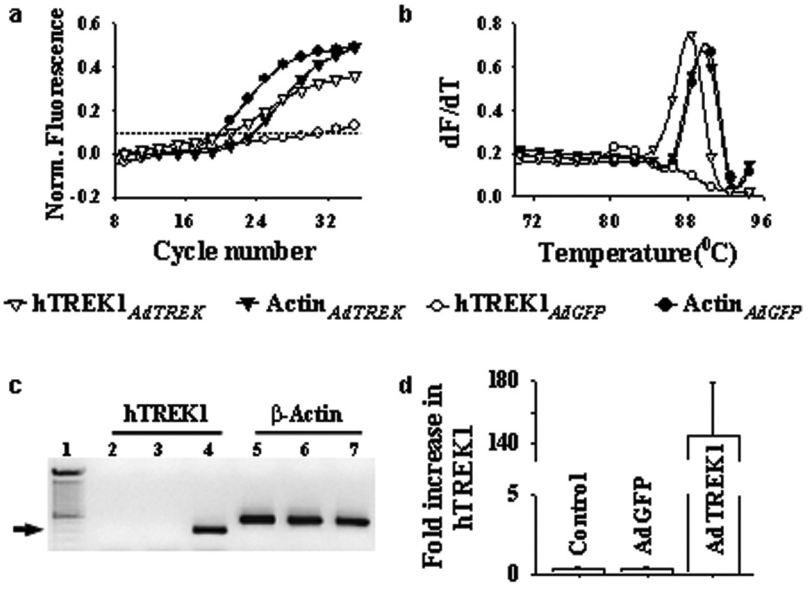

Fig. 1. mRNA expression of hTREK1 in Ad-hTREK1-infected HEK 293 cells. a, SYBR Green real-time PCR kinetic data traces for the genes hTREK1 and β-actin. Open symbols, cDNA from cells (Ad-GFP and Ad-hTREK1-infected) amplified with hTREK1 specific primer; closed symbols, cDNA from cells amplified with β-actin-specific primer. b, corresponding melting or dissociation curves of the real-time PCR products for the same reaction as described in a. c, specific amplification of hTREK1 in Ad-hTREK1-infected cells illustrated by 0.4-kilobase amplicon of hTREK1 gene (marked by arrow). Lane 1, 100-base pair marker; lanes 2 and 5, cDNA from uninfected HEK 293 cells; lanes 3 and 6, cDNA from cells infected with AdGFP; and lanes 4 and 7, cDNA from cells infected with Ad-hTREK1. d, -fold increase in the hTREK1 mRNA expression in Ad-hTREK1-infected HEK 293 cells as quantified from real-time PCR data.

current amplitudes at varying membrane potentials (Fig. 3c), which show the shift in reversal potential of hTREK1 from approximately −84 to 0 mV upon changing the external K^+ concentration from 2.5 to 150 mM. The above-mentioned observation confirms the K^+ selectivity of the hTREK1 channel isoform we used for our experiments. The slope conductance measured from the linear part of single channel I-V relation was found to be 95.7 ± 9.4 pS (n = 7), which is in agreement with previous observations (Bockenhauer et al., 2001; Honoré, 2007). It has been reported that alternative translation initiation leading to generation of splice variants with shorter N-terminal domains result in channels with variable conductance and increased permeability to Na^+ (Simkin et al., 2008; Thomas et al., 2008). However, in our hands, all the hTREK1 channel activities observed were K^+-selective and had similar single-channel conductance as mentioned above (Fig. 3c). Thus, the experimental results presented here on the effects of lidocaine on hTREK1 are probably on the single isoform of hTREK1 channels with an intact N-terminal domain (NTD). Human TREK1 is a known mechanosensitive channel. On application of negative pressure in excised patches, the open probability of single hTREK1 channels increased significantly (Fig. 3d). This was used as a positive test to identify the hTREK1 channels in excised patches.

Figure 4a illustrates the single hTREK1 channel activity elicited at −60 mV in control, in presence of lidocaine and after washout. It shows that lidocaine reversibly and in a concentration-dependent manner inhibits single hTREK1 channel activity. Inhibition was quantified by estimation of the NP_o, where P_o is the channel open probability and N is the number of channels in the patch (see *Materials and*

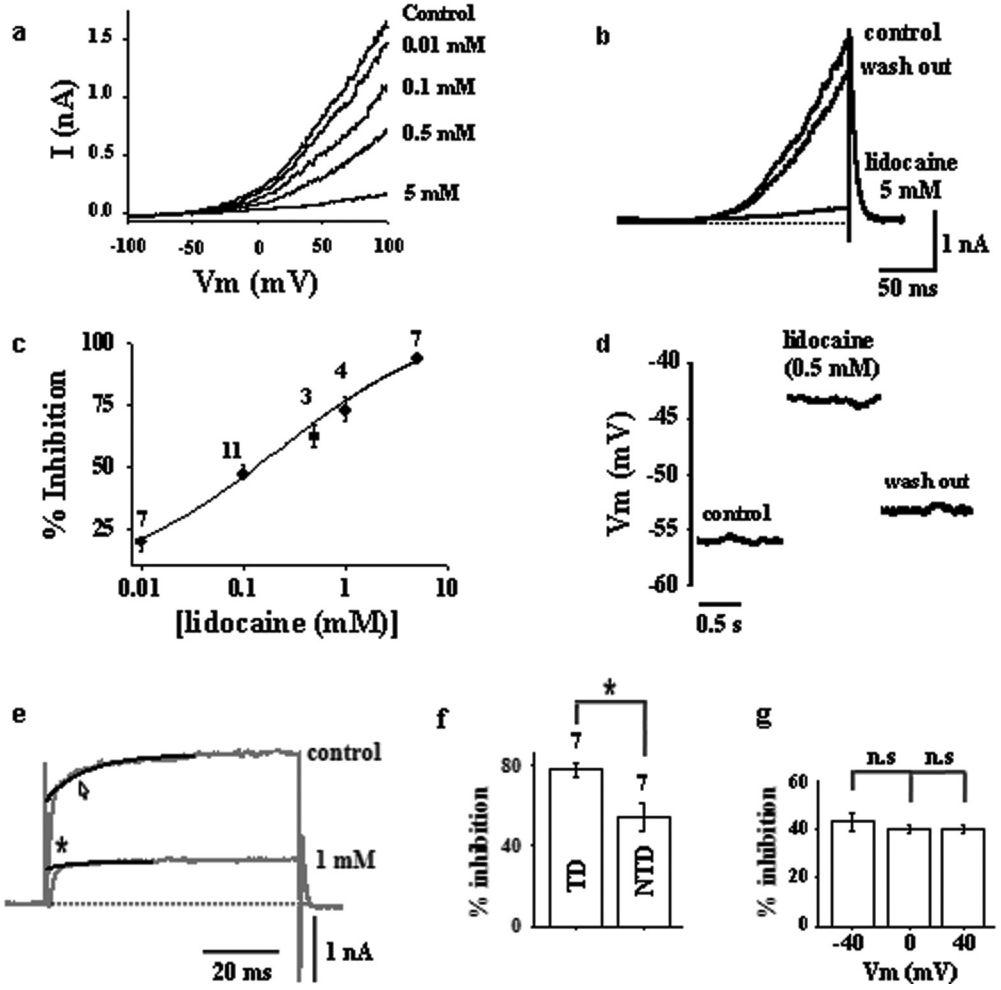

Fig. 2. Lidocaine inhibits whole-cell hTREK1 channel current. a, hTREK1 current evoked by ramp changes in voltage (−100 to 100 mV) in control condition and in the presence of increasing concentrations of lidocaine. The holding potential was −80 mV, and the test concentrations are illustrated. b, inhibition of hTREK1 current was reversible on washing out even a high concentration of lidocaine (5 mM), illustrated by raw current traces elicited by ramp voltage pulses as described in a. c, concentration-response curve for lidocaine inhibition of hTREK1 current. Numbers above the data points correspond to the number of cells tested for each concentration of lidocaine. d, current-clamp recordings of membrane potential of HEK 293 cells infected with Ad-hTREK1 under control condition, during application of 0.5 mM lidocaine, and after washout of the drug. Note the membrane depolarization and reversibility of the membrane potential upon washing out of lidocaine. e, lidocaine nonspecifically inhibits both the instantaneous (highlighted by asterisk) and time-dependent component (pointed by arrow) of whole-cell hTREK1 current (gray lines). Whole-cell current was evoked by rectangular 50-ms voltage pulse from −80 to 40 mV in absence (control) and presence of 1 mM lidocaine. The black curves superimposing the current traces represent the exponential function fitted to the activation time course. f, percentage inhibition of the time-dependent (TD) and non–time-dependent (NTD) components of hTREK1 current in presence of 1 mM lidocaine (∗, $p < 0.05$). g, lidocaine induced inhibition was independent of voltage. Voltage-dependent inhibition was analyzed by comparing percentage of inhibition in whole-cell steady-state current amplitudes at three different membrane potentials: −40, 0, and 40 mV, respectively, in the presence of 0.1 mM lidocaine. The difference in inhibition was not significant (n.s).

Methods). Figure 4, b and c, illustrates the reduction in channel activity in terms of NP_o at 100 μM and 5 mM lidocaine, respectively. The inhibition was rapid, with a 50% reduction in channel activity observed within 15.7 ± 5.1 s (n = 17) after treatment with 5 mM lidocaine. The average NP_o on application of 100 μM and 5 mM lidocaine has been illustrated as bar diagram showing the concentration dependence of hTREK1 inhibition and reversal of NP_o upon washing out lidocaine (Fig. 4d).

A decrease in channel NP_o by lidocaine could be because of an anesthetic-induced decrease in the mean open time (τ_o), an increase in the mean close time (τ_c), or both. The mean dwell times (τ_o, t_c) were estimated by fitting the dwell time distribution histograms by mixed exponential probability density functions (see *Materials and Methods*). The open time and close time distributions in our case were fitted by mono- and biexponential functions, respectively. It is interesting that the mean open time was found to be unaltered upon application of lidocaine (2.6 ± 0.8 ms for low and moderate concentrations of lidocaine, 100 μM in this case; n = 6), as illustrated in Fig. 5, a and b. However, the slow time constant of the closed state ($\tau 2_{close}$) significantly increased [control, 38.4 ± 24 ms; lidocaine (100 μM), 163.6 ± 57 ms; $p < 0.01$, Mann-Whitney U test; n = 6] in presence of lidocaine, whereas the fast time constant ($\tau 1_{close}$) was almost unaffected (control, 1.1 ± 0.32 ms; lidocaine, 0.89 ± 0.14 ms; $p > 0.05$, Mann-Whitney U test; n = 6) (Fig. 5, a and b). This may explain the reduced open probability of the channel in presence of lidocaine. In addition, in presence of low concentrations of lidocaine (100 μM), there was a marked reduction in the amplitude of the unblocked open conductance levels "O" of hTREK1 (O*, O; control, −2.4, and −5.7 pA; 100 μM lidocaine, −2.3 and −2.8 pA, respectively), although the unitary current amplitude remained largely unaltered, as illustrated by the amplitude histograms (Fig. 5c). At higher concentration of lidocaine (5 mM), the bursting behavior of hTREK1, observed in the absence of lidocaine (Fig. 3a), was abolished, where the inhibition could be mostly attributed to the drastic reduction in open probability of single hTREK1 channels (Fig. 4, c and d). However, upon washing out lidocaine, resumption of bursts and increase in the open probability, comparable with activity before application of lidocaine, could be observed (Figs. 4a and 5c).

Negative Cooperativity and Half-of-Sites Saturation Kinetics. The observation of negative cooperativity for the inhibition of hTREK1 by lidocaine at whole-cell level (Fig. 2C) could be due to negative cooperative interaction between the individual channels in the membrane (Hehl and Neumcke, 1993) or because of the intersubunit negative cooperativity, attributable to allosteric interaction of lidocaine with hTREK1 (Suzuki et al., 2004). To determine the source of negative cooperativity, we measured the response of single hTREK1 channels to a wide range of lidocaine concentrations in excised inside-out patches. The inhibitory effect of lidocaine was found to be concentration-dependent between the test range of 10 μM and 5 mM. The concentration-response data obtained from NP_o analysis were fitted to the Hill equation (see *Materials and Methods*). The IC_{50} value and the Hill

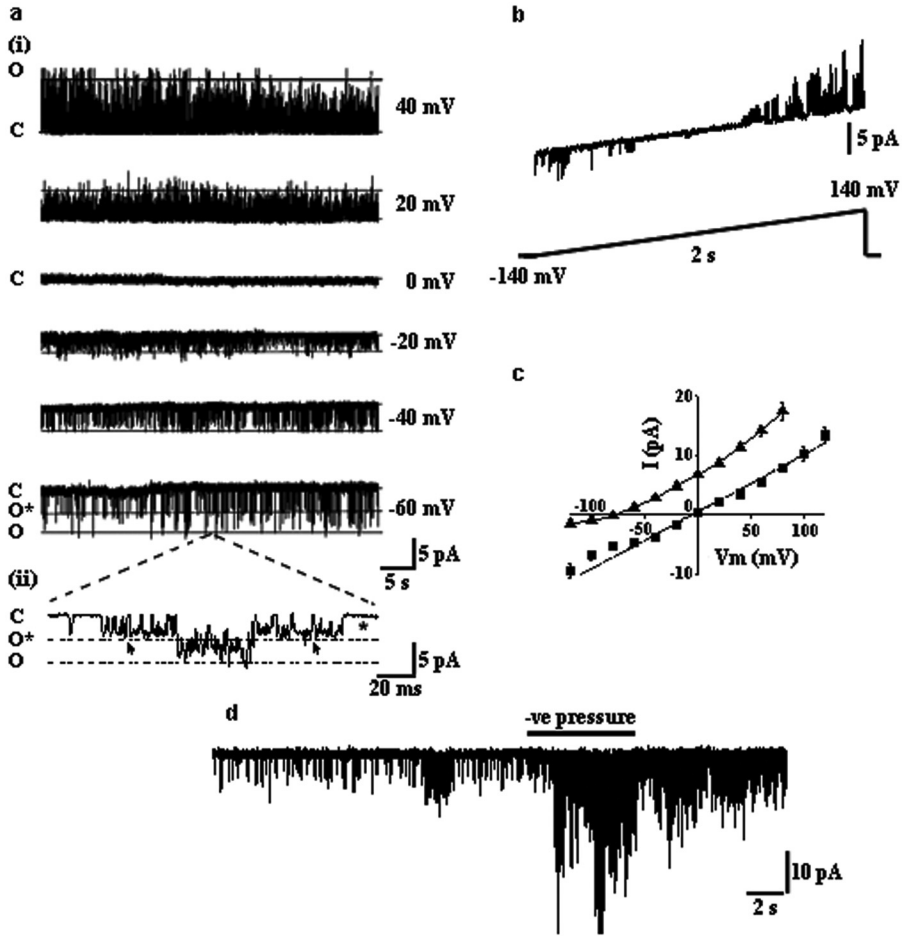

Fig. 3. Characterization of single hTREK1 channels in excised inside-out patches. a, i, a single hTREK1 channel at varying membrane potentials (as indicated) in symmetrical K^+ gradient showing reversal at 0 mV. Shown are the two open conductances, O* (blocked, −2.9 pA) and O (unblocked, 6.8 pA), at hyperpolarized potential (−60 mV) owing to the internal Mg^{2+} block. Note the mild outward rectification of single hTREK1 channel. ii, part of the trace at −60 mV, illustrated at high resolution. Note the presence of the two open conductance levels depicted by dotted lines. The arrow points to the flickery short-duration closed state within the burst, and the asterisk marks the long interburst closed state. b, single hTREK1 channel current evoked in symmetrical K^+ gradient by a ramp pulse depicted below the current tracing. c, single-channel current-voltage relationship obtained by measuring the unitary current amplitudes at varying potentials in symmetric and physiological K^+ gradients. The reversal potential of hTREK1 shifted from −84 to 0 mV on changing the external K^+. The measured slope conductance was 95.7 ± 9.4 pS (n = 7). d, TREK1 is a mechanogated channel. Note the prominent increase in open probability of hTREK1 on application of negative pressure through the patch pipette.

coefficient were estimated to be 171 ± 23 μM and 0.56 ± 0.11, respectively (Fig. 6a), which are not significantly different from the whole-cell data shown in Fig. 2C. Hill coefficient less than 1 suggests negative cooperativity in the interaction of lidocaine with the single hTREK1 molecule. Because in excised inside-out patches, we often observed activity of only a single channel molecule, it is imperative to suggest that lidocaine induced intersubunit negative cooperativity in the hTREK1 molecule. However, a possible existence of a cooperative interaction between individual channels could not be ruled out from our experiments.

The concentration-dependent reduction in NP_o of hTREK1 was also used to understand the kinetics of lidocaine interaction with the channel molecule. Assuming saturating ligand concentration, the interaction of lidocaine with hTREK1 was considered to follow pseudo–first-order kinetics. Pseudo–first-order rate constant K_i for the inhibition of hTREK1 at a given concentration of lidocaine was determined according to the following equation: $ln\ (NP_o/NP'_o) = -K_i \times t$, where NP'_o is the NP_o before lidocaine treatment and NP_o/NP'_o is the relative decrease in the NP_o after time t of lidocaine application. Figure 6b illustrates the plot of ln (NP_o/NP'_o) against time t (minutes), the slope of which gives an estimate of the pseudo–first-order rate constant K_i (minutes^{-1}) for a particular concentration of lidocaine (Wang and Wu, 1997). The kinetics of concentration-dependent inhibition was obtained by determining the reaction order of the pseudo–first-order reaction from the following equation: $K_i = K'_i \times [\text{lidocaine}]^n$, where K'_i is the second-order rate constant and n is the reaction order or the minimal number of lidocaine molecules involved in the interaction with the hTREK1 channel. This equation was further transformed into $\log(K_i) = n\ \log([\text{lidocaine}]) + \log(K'_i)$, which allows the estimation of the n parameter from the slope of the double logarithmic plot between K_i and concentration of lidocaine (Wang and Wu, 1997). Figure 6c shows the double logarithmic plot, from which the reaction order was determined to be 0.47 (~0.5) for the interaction of lidocaine with hTREK1. This suggests that the interaction of lidocaine with the channel molecule is unlikely to be a simple single-site binding reaction and involves more than one allosteric site. Stoichiometric half-reaction order (0.5) suggests that at steady state, only half of the allosteric sites on the hTREK1 molecule, which is a dimeric protein, are occupied by lidocaine. Thus, lidocaine apparently shows half-of-sites saturation kinetics in its interaction with hTREK1 (Fersht, 1975; Azurmendi et al., 2005). To verify the above-mentioned findings, we compared the kinetics of lidocaine inhibition of hTREK1 with that of a known activator of the channel, TCE, an active metabolite of the general anesthetic chloral hydrate (Harinath and Sikdar, 2004). TCE was found to potentiate hTREK1 activity in a dose-dependent manner, with an EC_{50} value of 230 ± 65 μM and the Hill coefficient of 1.6 ± 0.28, suggesting strong positive cooperativity in its interaction with hTREK1. In contrast, from a similar analysis as described above, we estimated the reaction order to be ~1.0

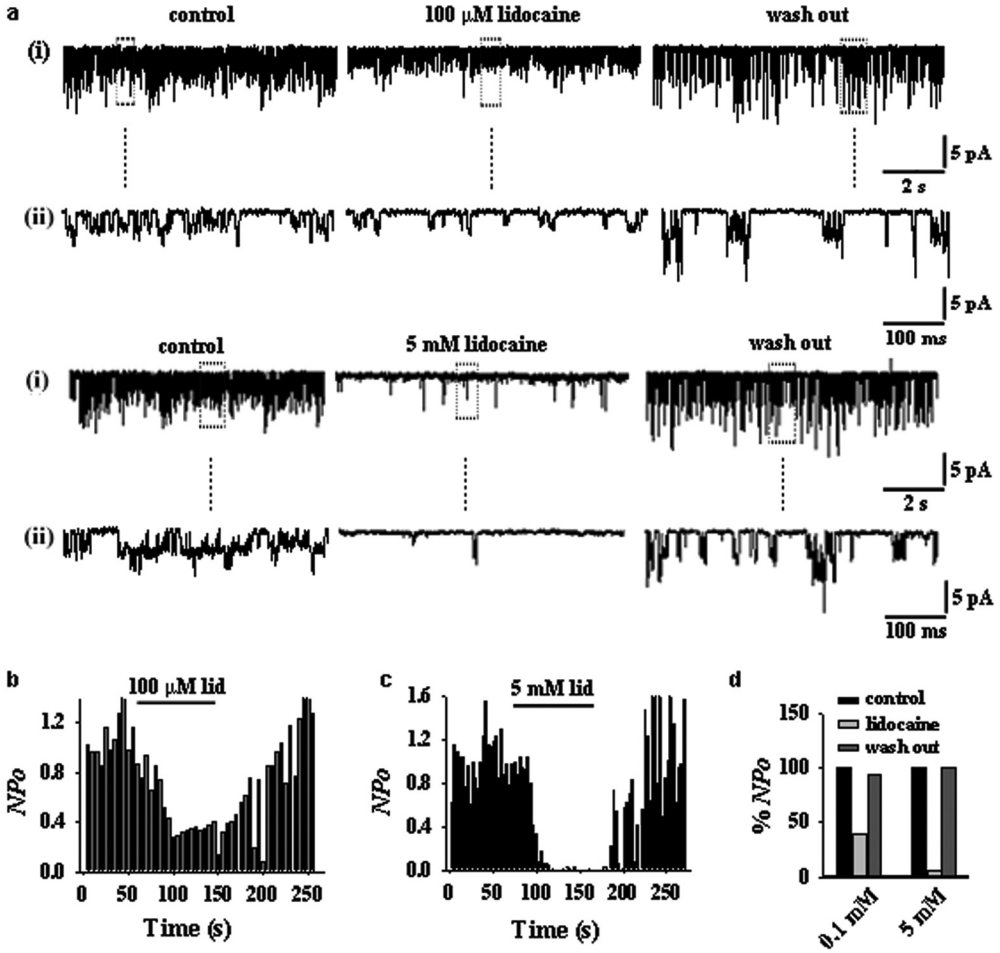

Fig. 4. Inhibition of single-channel hTREK1 current by lidocaine. a, i, single-channel current recordings obtained at −60 mV in excised inside-out configuration under control condition, during application of lidocaine [100 μM (top) and 5 mM (bottom)] and after washout. Note the concentration dependent reduction in open probability and absence of burst behavior of the channel upon application of lidocaine. ii, part of the traces highlighted by dotted boxes in i has been illustrated at higher time resolution. b, plot of hTREK1 NP_o from an excised inside-out patch in control condition, in the presence of 100 μM lidocaine and upon washout. The averaged NP_o was sampled every 5 s and plotted versus time (seconds). The horizontal bar represents the duration for which lidocaine was applied. c, plot of hTREK1 NP_o from the same patch as above under control condition, in presence of 5 mM lidocaine and upon washout. The averaged NP_o was sampled and plotted versus time (seconds) as described in b. The horizontal bar represents the duration for which lidocaine was applied. d, comparison of average NP_o of hTREK1 from the data in b and c in control conditions, in the presence of lidocaine, and upon washout. The concentrations of lidocaine used, are indicated in the figure.

(0.93) (Supplemental Fig. S2). Reaction order of 1 with respect to the ligand suggested a single-site binding of the TCE molecule to the hTREK1 channel. This comparative kinetics highlights the basic kinetic difference between an allosteric inhibitor and an allosteric activator of the channel molecule.

C-Terminal Domain of hTREK1 Mediates the Effect of Lidocaine. The positively charged quaternary ammonium analog of lidocaine, QX314 (5 mM), was found to have no effect on the hTREK1 current at whole-cell level ($n = 4$) (Fig. 7a). This suggests that lidocaine interacts with a domain of the hTREK1 channel that is accessible only from the intracellular side. The cytoplasmic CTD of TREK1 has been implicated in the sensitivity of the channel to several modulators, such as volatile anesthetics (Patel et al., 1999), stretch, temperature, and intracellular acidosis (Maingret et al., 1999; Honoré, 2007). Therefore, we evaluated the possible role of the CTD of hTREK1 in mediating the inhibitory effect of lidocaine by using C-terminal deletion mutants and single amino acid substitutions.

Deletion of the carboxyl-terminal 119 residues of hTREK1 (Δ119) (Fig. 7b) abolished the outward rectification property of the channel, whereas deletion of the distal 89 residues (Δ89; Fig. 7b) conferred only mild outward rectification (Fig. 7c). The whole-cell current density of both the deletion mutants, however, was not significantly different from the wild-type hTREK1 (Fig. 7d). It is interesting that both the C-terminal deletion mutants were completely insensitive to lidocaine. Figure 8a illustrates the comparison of the whole-cell current response of the wild-type hTREK1 and Δ119 and Δ89 mutants to ramp membrane potential from −80 to 80 mV in the presence of 5 mM lidocaine. The inset represents the time course of the effect of lidocaine on the whole-cell current. The percentage of inhibition observed in case of wild type (92.6 ± 5.9%; $n = 14$) is significantly higher ($p < 0.001$, Mann-Whitney U test) compared with Δ89 mutants (0.56 ± 5.7%; $n = 5$) and Δ119 mutants (−8.0 ± 13.9%; $n = 6$) as illustrated in Fig. 8b. The effect of lidocaine (5 mM) on the mutant Δ89 and Δ119 hTREK1 channels was also investigated at single-channel level in excised inside-out patches. Figure 8c illustrates the application of 5 mM lidocaine in an inside-out patch expressing Δ119 mutant, which showed mild increase in single-channel activity rather than inhibition. However, the change in current amplitude, open probability, and the burst behavior on application of lidocaine was insignificant. It was quantitatively expressed as the maximal open probability, NP_o of the mutant channel (Fig. 8d), which shows no significant variation upon application of lidocaine ($p > 0.05$, Mann-Whitney U test; $n = 5$) (Fig. 8d).

To map the region(s) responsible for lidocaine sensitivity in the C-terminal 89 residues, we incorporated point mutations in the CTD. The voltage-gated Na^+ channel is the known major target of local anesthetic molecules such as lidocaine. Alanine scanning mutagenesis has revealed a near universal importance of two strategically placed D4/S6 aromatic residues Phe1579 and Tyr1586 (Na_v 1.4 nomenclature) in the inhibition of voltage-gated Na^+ channels by class 1A and 1B (lidocaine belongs to 1B) antiarrhythmic drugs (Ragsdale et al., 1994; Nau and Wang, 2004; Ahern et al., 2008). Further studies also attribute a cation-π interaction to be the basis of lidocaine binding to this aromatic moiety (Ahern et al., 2008).

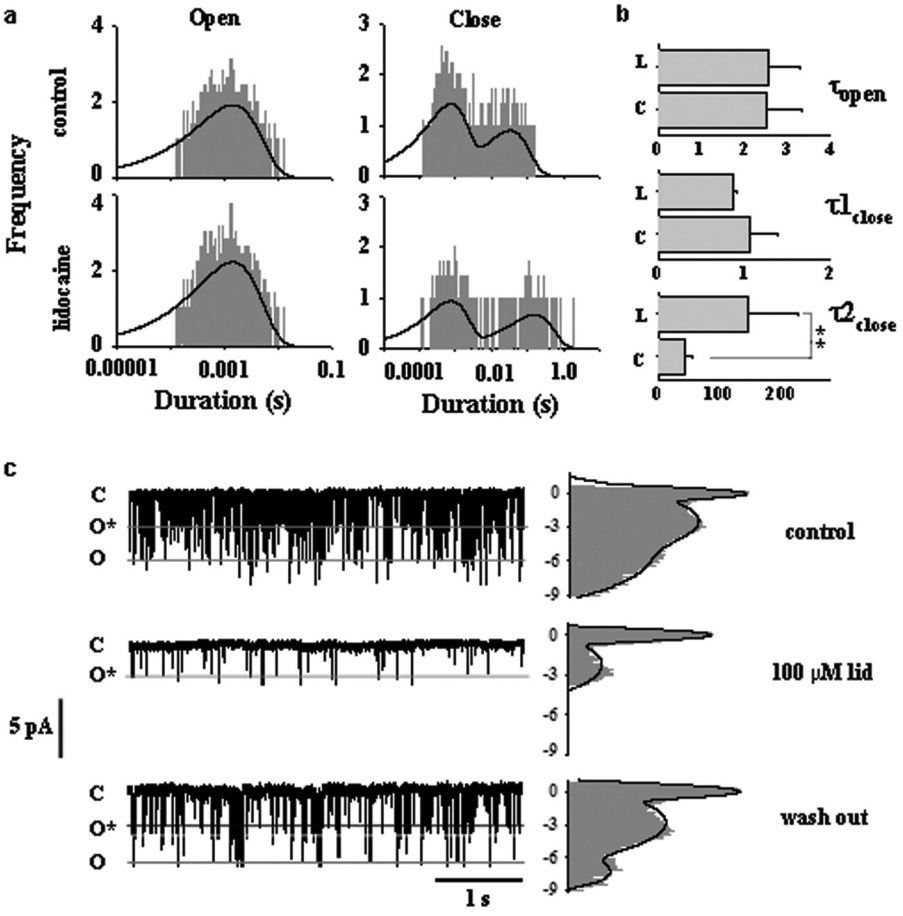

Fig. 5. Explanation for lidocaine induced inhibition of hTREK1 current from single-channel analysis. a, dwell time distribution histograms for the open and close times in the control (top) and in presence of 100 μM lidocaine (bottom) obtained from patches containing only one channel. The solid curves represent the probability density functions fitted to the histograms. b, comparison of mean dwell times (τ in milliseconds) in the control (C) and in the presence of 100 μM lidocaine (L) (**, $p < 0.01$). c, single-channel current evoked in control condition (top), in presence of 100 μM lidocaine (middle), and after washout (bottom), along with the corresponding amplitude histograms. Illustrated are the conductance levels C (close), O (open), and O* (horizontal bars in the current tracings) and the corresponding humps in the amplitude histograms. Note the reduction in current amplitude of the unblocked open level (raw data as well as amplitude histogram) upon lidocaine application though the unitary current remains unaltered.

It is interesting that we identified a subdomain in the CTD of hTREK1 between the PKA phosphorylation site Ser348 and cGMP-dependent kinase phosphorylation site Ser366, having two aromatic residues Tyr352 and Phe355, ideally placed to form a local anesthetic binding site (Fig. 7b, i). Multiple sequence alignment of the C-terminal domain of hTREK1 with the proposed local anesthetic binding region of Na_v channels from skeletal muscle (SCN4A) and the brain (SCN2A) show that the two aromatic residues Tyr352 and Phe355 along with the Ser348 residue seem to be conserved in Na_v channels (Fig. 7b, ii) despite a weak homology at other residues in the domain. On the contrary, we found that the human TREK2 channel, which shares more than 80% homology with hTREK1 in the C-terminal domain, does not have a homologous aromatic couplet in the vicinity of the Ser residue (Fig. 7b, iii). It was most surprising that human TREK2 has been shown to be nonresponsive to even 1 mM lidocaine (Bang et al., 2000). In contrast, Ser348, which determines the net charge in the subdomain depending on its phosphorylation state, may affect the strength of cation-π interaction of lidocaine. Therefore, to directly test the role of this subdomain, we used the mutations S348A, S348D, and S366A and the double mutant Y352A/F355A in the CTD. In our hands, all the above-mentioned mutations yielded functional channels that largely retained the properties of hTREK1 as illustrated in Fig. 7c (see Supplemental Fig. S3 for S366A). However, for the S348A mutant the basal current level significantly increased compared with wild-type hTREK1 and the S348D mutation led to expression of channels, with considerably lower current density (Fig. 7, c and d), as reported previously (Murbartián et al., 2005). Although the maximal inhibition (at 5 mM lidocaine) for the S348A mutant (phosphorylation-defective mutant) (86.2 ± 6.4%; $n = 8$) was not significantly different ($p > 0.05$, Mann-Whitney U test) from that of the wild-type hTREK1 (92.6 ± 5.9%; $n = 14$), the reversal of inhibition upon washing out lidocaine was considerably slower compared with the wild type (Fig. 8a, inset). In contrast, the constitutive phosphorylation mimicking mutant S348D exhibited a maximal inhibition of 41.4 ± 14.3% ($n = 5$) with 5 mM lidocaine, which was significantly less compared with that of the wild-type hTREK1 (92.6 ± 5.6; $n = 14$; $p < 0.01$, Mann-Whitney U test; $n = 5$). It is interesting that the reversal of inhibition in S348D was comparable with that of the wild-type hTREK1 (Fig. 8a, inset). To ascertain that the minimal inhibition of the S348D mutant channel by lidocaine is not an artifact masked by the reduction in the current density, we performed experiments by activating the mutant channels (both S348A and S348D) with arachidonic acid (AA; 1 μM) before the application of lidocaine (5 mM). The results illustrate a similar trend in inhibition as observed without AA. S348A mutant showed a greater inhibition, whereas S348D was mildly inhibited, although both of them showed marked potentiation after AA application, as illustrated in Fig. 9a.

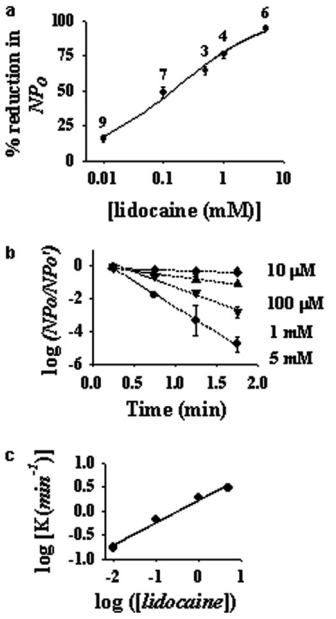

Fig. 6. Concentration-response and kinetic analysis of lidocaine binding to hTREK1. a, concentration-response curve of lidocaine inhibition fitted to the Hill's equation (see *Materials and Methods*). The estimated Hill's coefficient was 0.57 (<1), suggesting negative cooperativity. Note the mild concavity in the log-linear plot, which is a signature of negative cooperativity. Numbers above the graph correspond to the number of cells tested for each concentration of lidocaine. b, lidocaine-induced decrease in NP_o of hTREK1 channel as a function of time. Each data point represents the mean NP_o during 30-s (0.5-min) recording periods. Pseudofirst-order rate constants K_i (minutes^{-1}) for the inhibition were determined from the slope of the plot as described in the text (see *Results*). c, double logarithmic plot between the pseudofirst-order rate constant K_i (minutes^{-1}) and concentration of lidocaine for determining the kinetic order of the reaction between lidocaine and the hTREK1. The slope of the double-logarithmic plot gives an estimate of the order of the reaction with respect to lidocaine.

To further verify the role of phosphorylation in the interaction of lidocaine with the channel, we performed experiments with the PKA activator forskolin and inhibitor KT 5720. On application of forskolin (1 μM), the hTREK1 current gradually decreased (over 3–5 min) and upon application of lidocaine (5 mM), there was a further mild inhibition (37.4 ± 5.3%; $n = 3$) over the steady-state phosphorylated current level, as shown in Fig. 9b, i. In contrast, incubation of cells with KT 5720 (1 μM for 10 min), the PKA inhibitor, led to drastic increase in hTREK1 current with time, which was almost completely inhibited by 5 mM lidocaine (87.2 ± 4.5% over the steady-state dephosphorylated current level; $n = 3$; data not shown). The reversal from inhibition, however, was gradual, similar to the phosphorylation-defective mutant S348A (Fig. 8a). Phosphorylation of Ser348 by PKA regulates the basal level current of hTREK1 (Bockenhauer et al., 2001), as shown in our experiments. It is most interesting that the S348A mutant of hTREK1 was unaffected by forskolin (1 μM) as shown in Fig. 9b, ii, which suggests that the Ser348 indeed gets phosphorylated by PKA activity. In essence, phosphorylation at Ser348 interferes with lidocaine induced inhibition, whereas dephosphorylation or incorporation of a hydrophobic residue (S348A) at the same site stabilizes the inhibited state and delays the reversal from inhibition.

However, the S366A mutation seemed to have no effect on lidocaine-mediated inhibition of hTREK1 (87 ± 5.4%; $n = 4$) (Supplemental Fig. S3, e and f). On the contrary, in the double mutant Y352A/F355A, replacement of the aromatic residues with alanine drastically hampered lidocaine-mediated inhibition (maximal inhibition, 13.4 ± 6.0% with 5 mM lidocaine; $n = 9$), as illustrated in Fig. 8, a and b. In excised inside-out patches, the double mutant behaved similar to that of the wild type, with two distinguishable open conduc-

tance levels and open channel bursts (Fig. 8e). Upon application of lidocaine (5 mM), however, there was no significant change observed compared with untreated wild-type channel (Fig. 8e). The mutant channel activity was quantified as the change in NP_o, which was not significantly different from the untreated channel activity ($p > 0.05$, Mann-Whitney U test; $n = 4$) (Fig. 8f). The above-mentioned results suggest that the two aromatic residues Tyr352 and Phe355 are instrumental in mediating the inhibitory effect of lidocaine and phosphorylation state of the Ser348 residue plays a key role in determining the inhibitory effect of lidocaine.

Intermediate Kinetics of the Heterodimer of Wild-Type hTREK1 and Δ119 Deletion Mutant Shed Light on the Reaction Mechanism. Transfection of equimolar ratio of the wt-hTREK1 and Δ119 cDNA in HEK 293 cells should result in expression of three distinct species of channels: homodimer of wild-type $hTREK1_{wt}$, homodimer of Δ119, and heterodimer of wt-hTREK1 and Δ119 (Czirják and

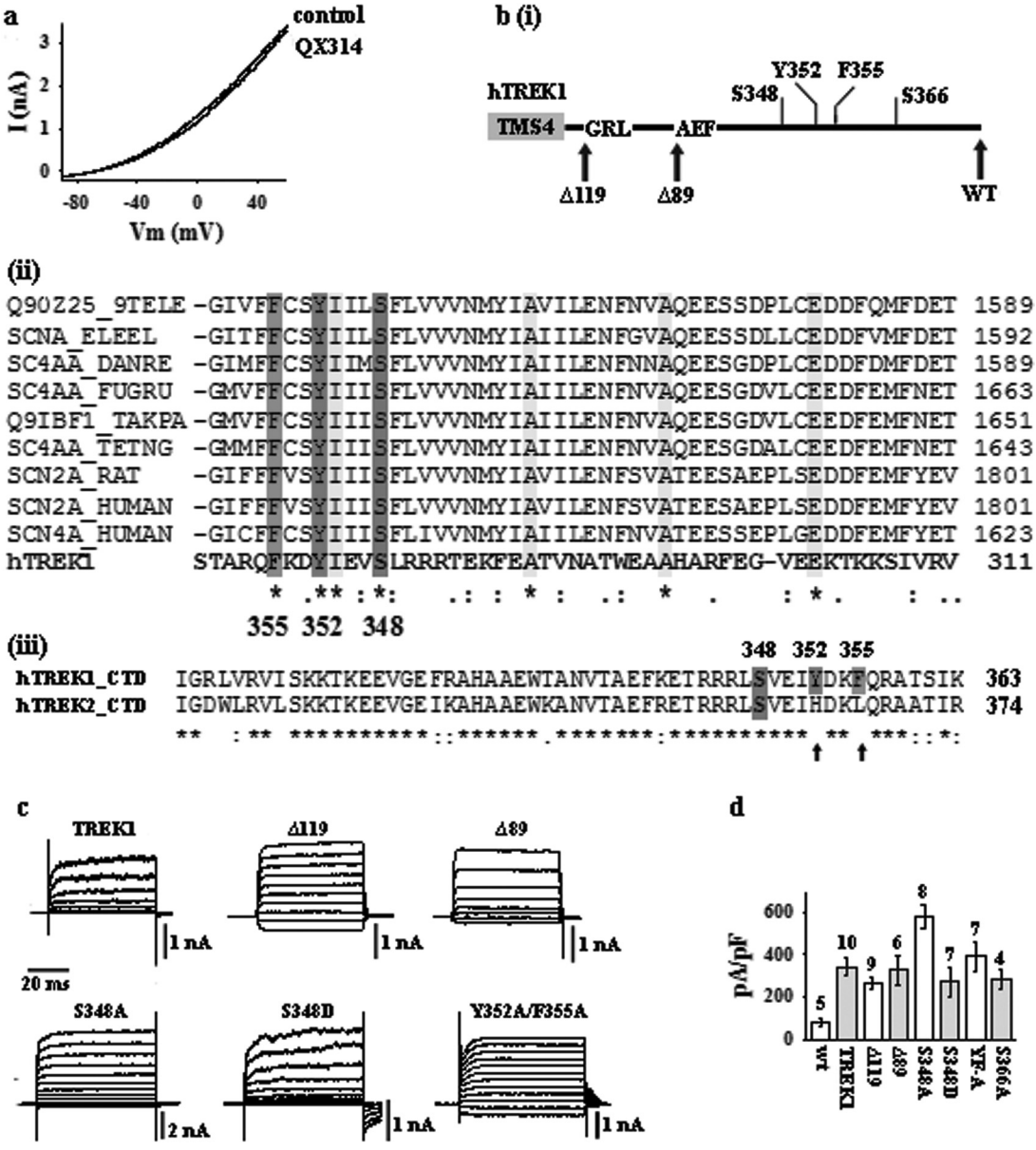

Fig. 7. Mapping of the lidocaine binding site in the C-terminal domain of hTREK1. a, QX314 (5 mM), a positively charged quaternary lidocaine derivative, has no effect on hTREK1 currents. Whole-cell current evoked from a holding potential of −80 mV by a voltage ramp from −100 to 60 mV. The difference in current with and without QX314 at 60 mV was insignificant ($p > 0.05$, Mann-Whitney U test; $n = 4$). b, i, cartoon representation of the C-terminal domain of hTREK1 illustrating the deletions and point mutations. The amino acid residues at the beginning of deletions (G and A), the phosphorylation sites (S), and the aromatic couplet (Tyr and Phe) are indicated. ii, multiple sequence alignment of the domain of CTD encompassing Ser348, Tyr352, and Phe355, with the proposed lidocaine binding domain of SCN4A and SCN2A from various origins. The highlighted regions represent the conserved residues. iii, pairwise alignment of the CTD of hTREK1 and hTREK2. The asterisk (*) represents the identical residues in the sequence, whereas the arrows indicate the absence of the residues Tyr and Phe in the hTREK2 CTD. c, whole-cell current profiles of wt-hTREK1 and mutant hTREK1 channels. Note the difference in the rectification properties and maximum steady-state current amplitudes (different y-scale bars) of the wt-hTREK1 and mutant channels. The whole-cell current was elicited by step pulses (−100 to 60 mV) from a holding potential of −80 mV. d, comparison of whole-cell current densities (pA/pF) of hTREK1 and mutants of hTREK1 expressed in HEK 293 with that of untransfected HEK 293 (wt). The numbers on the bars depict the number of cells tested.

Enyedi, 2002). Consistent with this, we observed three different populations of channels constituting the whole-cell current obtained from HEK 293 cells transfected with wt-hTREK1 and Δ119 cDNA. The whole-cell current profile from such cells was intermediate between that of wt-hTREK1- and Δ119 homodimer-expressing cells. The whole-cell current was mildly outwardly rectifying as illustrated in Supplemental Fig. S3, a and b. The time-dependent component of the whole-cell current was estimated from the ratio of the steady-state current (I_{st}) to the current at time 0 (I_0) (Maingret et al., 2002). Cells expressing both the wt-hTREK1 and Δ119 exhibited intermediate time dependence (I_{st}/I_0 = 1.4 ± 0.2 compared with 1.95 ± 0.12 for wt-hTREK1 and 1.1 ± 0.1 for Δ119, n = 4) (Supplemental Fig. S3c). The three populations became more apparent on application of lidocaine by virtue of their differential response to lidocaine. Figure 10a illustrates the time course of the whole-cell current response of cells expressing wt-hTREK1, Δ119 alone, and cells expressing both of them. The maximal steady-state inhibition observed in cells expressing the heterodimer $hTREK1_{wt}$-Δ119 was 54.8 ± 9.9 (n = 6), which is intermediate between wt-hTREK1 (92.6 ± 5.9%; n = 8) and Δ119 mutant (−8.0 ± 13.9%; n = 5), as illustrated in Fig. 10d. The inhibition time course (Fig. 10a) was fitted with exponential functions (see *Materials and Methods*) to obtain the mean decay times. In wild-type hTREK1, the decay could be fitted to a single exponential with time constant 18.8 ± 5.0 s (n = 6), whereas in cells expressing $hTREK1_{wt}$-Δ119, the decay had two exponential components with time constants, $\tau 1$ = 16.6 ± 12.6 s and $\tau 2$ = 170.2 ± 65.4 s (n = 4) (Fig. 10b). The fast inhibition

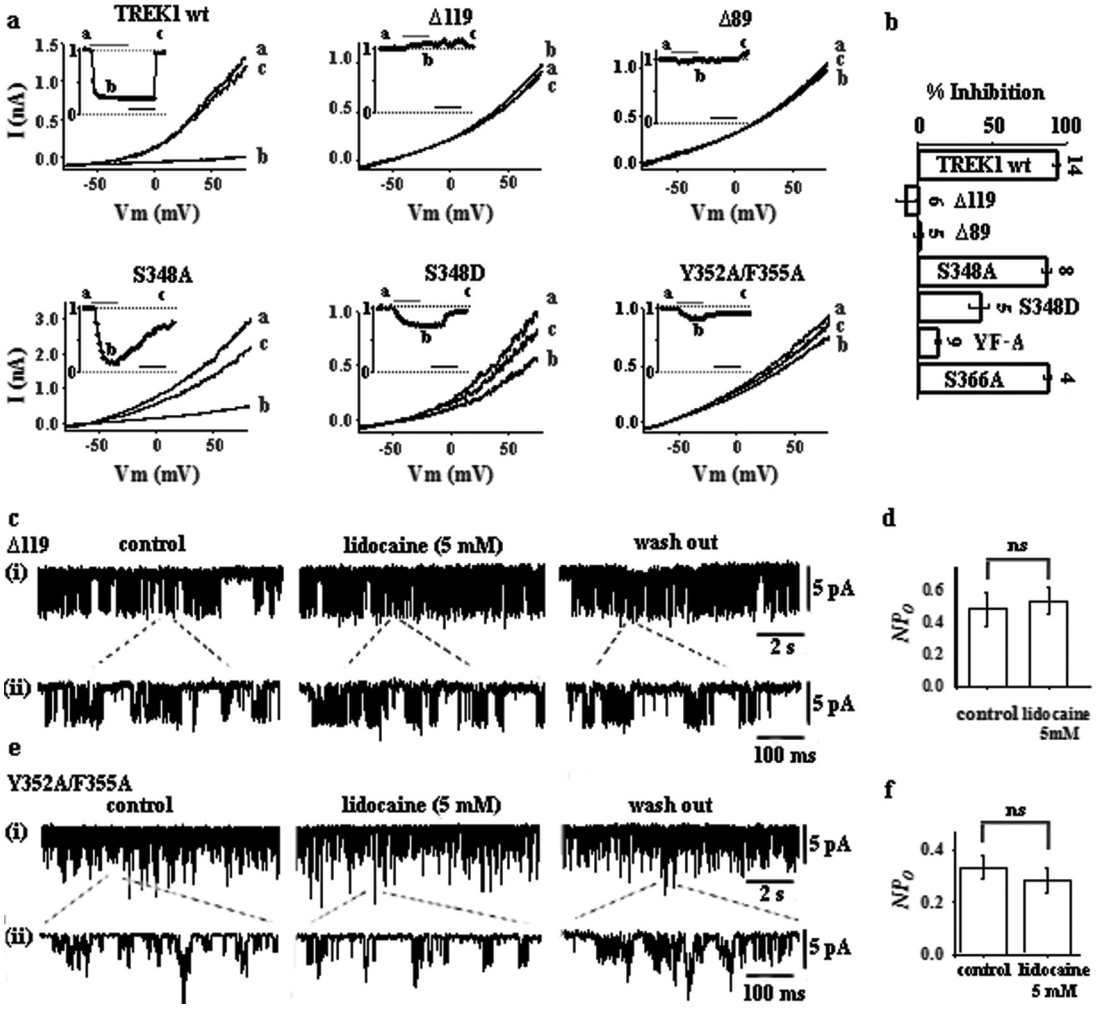

Fig. 8. Analysis of the C-terminal domain mutants reveal the binding site for lidocaine. a, whole-cell current recorded from HEK 293 cells expressing wt-TREK1, C-terminal deletion mutants Δ119 and Δ89 hTREK1, point mutants S348A and S348D, and the double mutant Y352A/F355A of hTREK1 by application of voltage ramp from −80 to 80 mV. a, steady-state current before application of lidocaine; b, steady-state current after application of 5 mM lidocaine; c, current after washout of lidocaine. Inset represents the time course of inhibition of whole-cell current (normalized) by lidocaine. a, b, and c on the time course represent the time points where the whole-cell currents were sampled and displayed. The x-axis scale bar of the inset is 100 s, and the horizontal bars above the time course represent the duration of lidocaine application. b, percentage inhibition of the whole-cell current upon application of lidocaine (5 mM) expressed as mean ± S.E.M. The numbers represent the number of cells tested. c, i, single-channel current traces recorded in inside-out configuration from a patch containing C-terminal deletion mutant Δ119 hTREK1 at −60 mV in control, during application of 5 mM lidocaine and after washout. Note that the single-channel current remains unchanged in presence of high concentration of lidocaine. ii, part of the trace in i has been illustrated in high resolution. Note the difference in time scale. d, comparison of average NP_o observed in control and in presence of 5 mM lidocaine. Data presented as mean ± S.E.M.; n.s, not significant. e, i, single-channel current traces recorded in inside-out patch expressing the double mutant Y352A/F355A as described above. ii, part of the trace in i has been illustrated in high resolution as above. Single-channel current was virtually unaffected in case of the mutant. f, comparison of average NP_o observed in control and in presence of 5 mM lidocaine on this patch. Data are presented as mean ± S.E.M.; n.s, not significant.

corresponds to the wt-hTREK1, the uninhibited component corresponds to the population of Δ119 mutant, and the slower inhibition is presumably due to the population of heterodimers of wt-hTREK1 and Δ119. This was further supported by excised inside-out single-channel recordings from cells expressing both wt-hTREK1 and Δ119. We observed three distinct classes of single-channel activities that exhibited different sensitivities to lidocaine (5 mM), as illustrated in Fig. 10c. They were distinguished by the percentage reduction in their NP_o value (Fig. 10e). The channels with intermediate sensitivity to lidocaine (percentage of reduction in $NP_o = 51.6 \pm 10.5$; three of 11 patches) was significantly different from channels with high sensitivity to lidocaine (percentage of reduction in $NP_o = 87 \pm 8.2$; five of 11 patches) and those that are insensitive to lidocaine (percentage of reduction in $NP_o = -2.6 \pm 12.3$; three of 11 patches). These channels represent the population of heterodimers of wt-hTREK1 and Δ119. These results suggest that coexpression of wt-hTREK1 and Δ119 leads to expression of a distinct population of heterodimers which exhibit partial inhibition upon lidocaine treatment. It further highlights the fact that the C-terminal domain is essential for lidocaine mediated inhibition, but a single C-terminal domain is not sufficient for maximal inhibition observed in wt hTREK1.

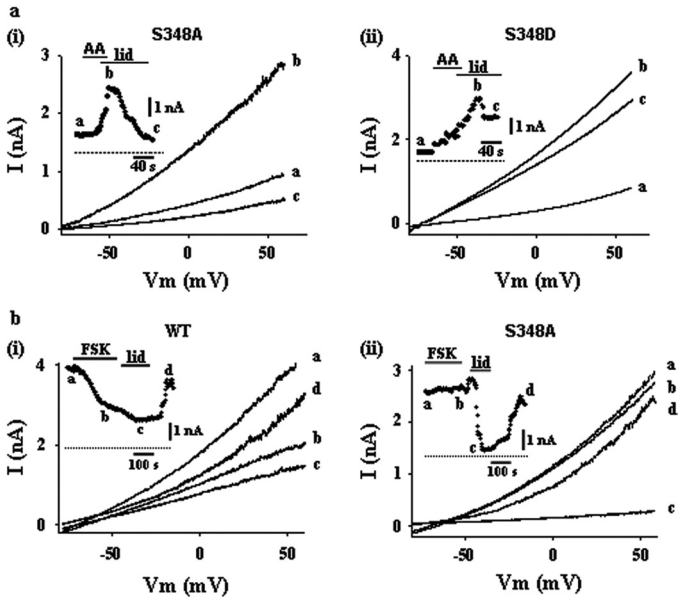

Fig. 9. Effect of lidocaine on hTREK1 (wt and mutant) after activation by arachidonic acid and forskolin (PKA activator). a, whole-cell current recorded from HEK 293 cells expressing the phosphorylation-defective mutant S348A (i) and the constitutive phosphorylation mutant S348D (ii) by application of voltage ramp from −80 to 60 mV. In both cases, a, the current before application of lidocaine; b, the current after application of 1 μM arachidonic acid; and c, the current after application of 5 mM lidocaine. Inset in both i and ii represents the time course of inhibition of whole-cell current (at 40 mV) by lidocaine. a, b, and c on the time course represent the time points where the whole-cell currents by applying voltage ramps were sampled and displayed. b, whole-cell current recorded from HEK 293 cells expressing wt-hTREK1 (i) and the phosphorylation-deficient mutant of hTREK1 S348A (ii) by application of voltage ramp from −80 to 60 mV on application of lidocaine followed by PKA activator forskolin. In both i and ii, a, the current before application of forskolin; b, the current after application of 1 μM forskolin; c, the current after application of 5 mM lidocaine after application of forskolin; and d, current after washing out both lidocaine and forskolin. Inset in both i and ii represents the time course of inhibition. a, b, c, and d on the time course represent the time points where the whole-cell currents to voltage ramps were sampled and displayed.

Discussion

The present study investigated the inhibitory action of lidocaine on the human K_{2P} channel TREK1. We report a unique aromatic couplet (Tyr and Phe) in the vicinity of the PKA phosphorylation site in the CTD of hTREK1 that is critical for the action of lidocaine on hTREK1. Furthermore, we elucidate a novel kinetic paradigm, involving intersubunit negative cooperativity and half-of-sites saturation of the allosteric sites, for this class of amide local anesthetics.

Inhibition of hTREK1 by Lidocaine: Role of Phosphorylation and the Aromatic Couplet in the CTD. Lidocaine inhibited the hTREK1 channel reversibly and in a dose-dependent manner, both at whole-cell and single-channel level (IC_{50} of ~180 μM) (Figs. 2c and 6a). In physiological condition, whole-cell hTREK1 current exhibited a leak or instantaneous component and a time-dependent component owing to the differential distribution of channels between two functionally distinct closed states, C_1 and C_2 (Kennard et al., 2005). The instantaneous component of the whole-cell current represents channels in C_2 moving to the single open state, O, whereas the time-dependent component represents channels moving more slowly from the resting closed state C_1 to O. Because lidocaine inhibits both the components of the whole-cell current (Fig. 2f), we propose that lidocaine binds nonspecifically to both the closed states of the channel. In contrast, at the single-channel level, the mean close time ($\tau 2$) for the long closures increased significantly (Fig. 5b) in presence of lidocaine, whereas the mean open time and the unitary current amplitude of hTREK1 were unaffected (Fig. 5, a and c). The increase in the mean close time is due to the appearance of more frequent long close events upon treatment with lidocaine. The frequency and duration of long-lived closed state depend on the stabilization of the closed state and have been implicated in the regulation of gating of the leak K^+ channels (Zilberberg et al., 2001; Ben-Abu et al., 2009). The above-mentioned evidence suggests that lidocaine stabilizes the closed state to manifest its inhibitory action on the channel.

Modulation of single-channel kinetic properties by lidocaine in excised inside-out patches and our work with the permanently charged analog of lidocaine QX314 (Fig. 7a) suggested that lidocaine interacts with the channel from the intracellular side. Furthermore, our studies with the deletion mutants revealed that the inhibitory effect of lidocaine was abolished in the C-terminal deletion mutants of hTREK1 (Δ89 and Δ119) (Fig. 8), underlining the importance of the CTD in mediating the effect of lidocaine. On further analysis of the CTD, we identified two strategically placed unique aromatic residues, Tyr352 and Phe355, in the vicinity of the PKA phosphorylation site Ser348, which were analogous to the aromatic couplet implicated in the interaction of lidocaine with voltage-gated Na^+ channels (Ragsdale et al., 1994; Nau and Wang, 2004; Ahern et al., 2008). It is interesting that the double alanine-substitution mutant of the aromatic couple, Y352A/F355A, abolished the inhibitory effect of lidocaine on hTREK1, both at the whole-cell and single-channel level (Fig. 8, b and f), analogous to the finding in Na_v channels. It is surprising that hTREK2, which is insensitive to high concentration of lidocaine (Bang et al., 2000), lacks the two aromatic residues despite sharing high homology with the hTREK1 CTD (Fig. 7b, iii). Thus, this aromatic couplet

might be an indispensable component of the lidocaine binding site in hTREK1. Further evidence in favor of a distinct lidocaine binding site came from the mutagenesis studies of the PKA phosphorylation site Ser348, which suggests that the presence of a charged moiety at this site reduces the inhibitory effect of lidocaine by destabilizing the inhibitory complex. In essence, the subdomain encompassing Ser348 to Phe355 is critical for the interaction of lidocaine with hTREK1, where the phosphorylation state of Ser348, in conjunction with the aromatic couplet, determines the binding efficacy of lidocaine. Because the presented results are from an isoform of hTREK1 with an intact NTD and because the N terminus is not involved in mediating the effect of anesthetics (Patel et al., 1999) and other ligands (Thomas et al., 2008), we conclude that the inhibitory effect of lidocaine is mediated by the CTD of hTREK1 independently of the NTD. Moreover, the ability of lidocaine to affect channel gating by binding to a site in the CTD qualifies it as an allosteric inhibitor of the hTREK1 channel.

Intersubunit Negative Cooperativity and Half-of-Sites Saturation Binding Kinetics. From the concentration-response curve of lidocaine binding to hTREK1, we estimated the Hill coefficient to be 0.49 (<1), which suggests that the interaction of lidocaine with the channel is strongly negatively cooperative. Negative cooperativity in ion channels is a fairly common phenomenon in allosteric antagonism and has been attributed to interaction between individual ion channels (ATP-sensitive-K^+ channels; Hehl and Neumcke, 1993), identical monomers (metabotropic glutamate receptor; Suzuki et al., 2004), and independent binding sites on the channel having different affinities for the ligand (connexin40 gap junction channels; Lin and Veenstra, 2007). We observed strong negative cooperativity in the interaction of lidocaine with single hTREK1 channel in excised inside-out patches (Fig. 6a), which largely eliminates the possibility of any allosteric interaction among individual channels. TREK1 is a homodimeric protein with two identical CTD, which serve as the docking sites for lidocaine. Because the CTD deletion and the Y352A/F355A double mutant of hTREK1 were predominantly insensitive to lidocaine, we rule out the possibility of other allosteric sites having differential affinities for lidocaine. Therefore, we conclude that lidocaine-induced negative cooperativity is the result of intersubunit interaction within the hTREK1 molecule.

A limiting case of negative cooperativity, where only half of the allosteric binding sites are occupied by ligands, has been described as the "half-of-sites binding stoichiometry" and has been known to facilitate the inhibitory action of antagonists (Fersht, 1975). Our finding of half-reaction order (0.47) with respect to lidocaine in the pseudofirst-order reaction involving lidocaine and the channel (Fig. 6c) suggested that only one molecule of lidocaine binds to hTREK1 homodimer, despite the availability of two structurally identical CTD. Thus, the reaction followed the half-of-sites saturation binding kinetics. Our studies with the heterodimer $hTREK1_{wt}$-Δ119 illustrated that the single CTD of the heterodimer is capable of mediating partial inhibition by lidocaine, but for complete inhibition both the intact CTD are essential (Fig. 10). It further emphasizes the fact that each of the CTD of hTREK1 is an independent binding site of lidocaine but that complete inhibition necessitates the cooperative interaction between both the CTDs upon lidocaine binding. In contrast, TCE binding to the channel molecule seemed to be a simple single-site binding (reaction order with respect to TCE was ~1.0) (Supplemental Fig. S2), which confirms that the half-of-sites

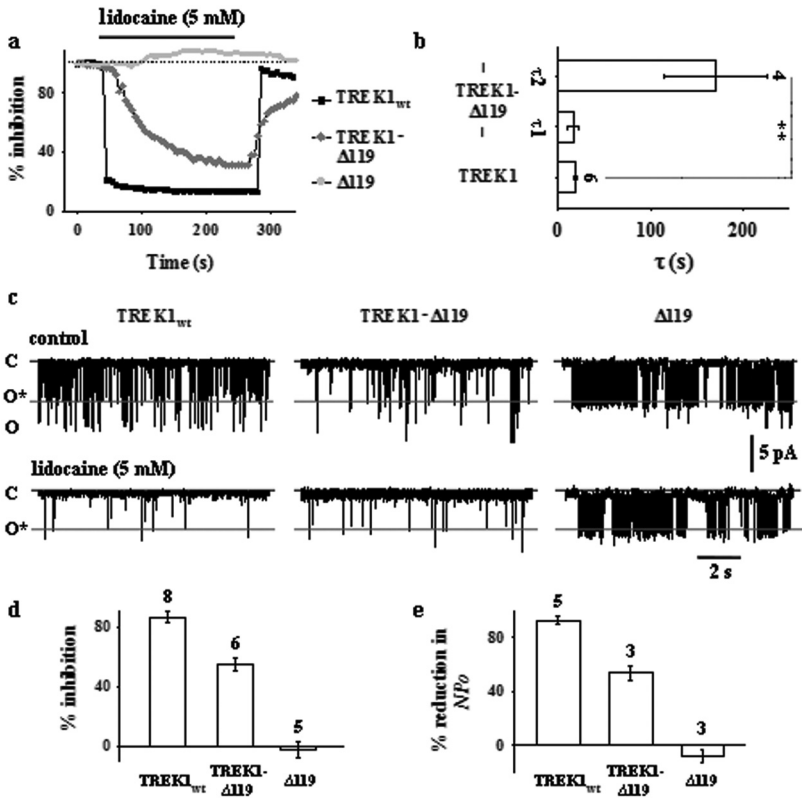

Fig. 10. Kinetics of the heterodimer of wt-hTREK1 and Δ119 mutant. a, the typical time course of the whole-cell response (normalized) of cells expressing hTREK1, Δ119 hTREK1, and equimolar ratio of both cDNA ($hTREK1_{wt}$-Δ119). Note the intermediate response of $hTREK1_{wt}$-Δ119 cells. The horizontal bar represents the duration of lidocaine (5 mM) application. b, the mean decay times (τ) obtained from the exponential fits of the inhibition time course (a) of hTREK1 and $hTREK1_{wt}$-Δ119 cells. **, $p < 0.01$. c, single-channel response from patches expressing the homodimer hTREK1, Δ119 hTREK1, and heterodimer $hTREK1_{wt}$-Δ119 in control condition (top) and after application of 5 mM lidocaine (bottom). Note the drastic reduction in open events in case of hTREK1, and the moderate effect of lidocaine on the heterodimer, whereas the Δ119 CTD mutant seemed to be insensitive to lidocaine. Also note that the unblocked open state "o" is absent in the homodimer Δ119 mutant but is rescued in the heterodimer. d, percentage inhibition of whole-cell current obtained from cells in a, presented as mean ± S.E.M. The numbers on the bars represent the cells tested. e, percentage inhibition of the maximal NP_o obtained from patches in c, presented as mean ± S.E.M. The numbers on the bars represent the cells tested.

binding stoichiometry is specific to the interaction of lidocaine and the CTDs of hTREK1.

A Model Explaining the Simultaneous Observation of Negative Cooperativity and Half-of-Sites Saturation Kinetics. Both negative cooperativity and half-of-sites binding stoichiometry are generally accompanied by ligand-induced structural asymmetry in multisubunit proteins (Azurmendi et al., 2005). To explain the above-mentioned two phenomena in lidocaine interaction with hTREK1, we propose a kinetic model, adapted from the studies of the enzyme tyrosyl-tRNA-synthetase (Fersht, 1975). We propose that binding of two lidocaine molecules, one lidocaine to each of the identical CTD would probably result in steric clash in the transient two lidocaine molecules plus channel complex as shown in Fig. 11a, i, which immediately disintegrates to give rise to a more stable hTREK1-lidocaine inhibitory complex having only one lidocaine bound to the channel (Fig. 11a, ii). In the kinetic model presented in Fig. 11b, k_2 is the apparent rate constant for formation of the transient partial inhibitory complex ($[T.L]_i$), and $k_1' \ll k_2'$, and k_2' as the binding of second lidocaine molecule to TREK1 is highly unfavorable. This explains the rapid formation of the stable inhibitory complex containing only one lidocaine, shown in Fig. 11b (Fersht, 1975). The present model is only descriptive in nature where the rate constants involved in the kinetic scheme have not been estimated. However, it satisfactorily explains both the negative cooperativity and the half-reaction order observed in our case. Results with the hTREK1 heterodimer $hTREK1_{wt}$-Δ119 (Fig. 10) suggests the existence of the partial inhibitory complex ($[T.L]_i$). Nevertheless, negative cooperativity has an important physiological implication in extending the lidocaine concentration range to which the hTREK1 molecule responds such that substantial amount of inhibition can be observed even at very low concentrations of lidocaine (Suzuki et al., 2004).

In various clinical settings, the plasma concentration of lidocaine can range from 20 to 30 μM to as high as 10 mM (Johnson et al., 2004). Because we observed significant block of hTREK1 even at very low concentrations of lidocaine (10 μM), TREK1 block might have important clinical consequences. Moreover, inhibition of leak K^+ channels increases membrane excitability (Drachman and Strichartz, 1991), which could explain the adverse neurological symptoms (Benkwitz et al., 2003) of lidocaine.

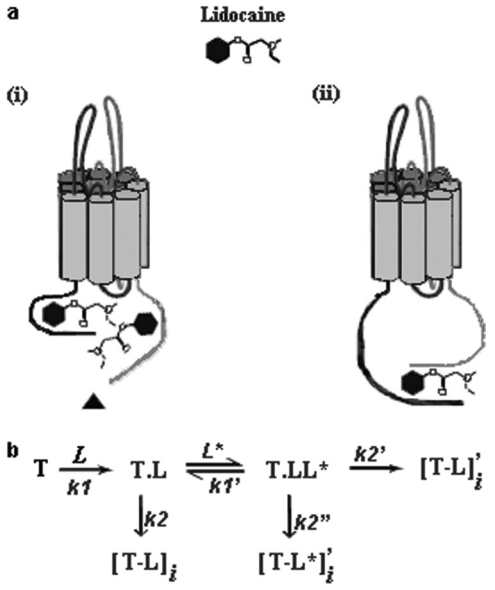

Fig. 11. Model explains the inhibition of hTREK1 by lidocaine. a, schematic representation of lidocaine binding to hTREK1. i, model of hTREK1 bound to two molecules of lidocaine at the CTDs. Note the strong steric inhibition for the binding of the second lidocaine molecule due to negative cooperativity. ii, model illustrating the stable inhibitory complex of hTREK1 and one molecule of lidocaine after the second lidocaine uncouples from the unstable complex in i, leading to half-of-sites saturation kinetics. b, kinetic model explaining both negative cooperativity and half-reaction order or half-of-sites reaction stoichiometry. In the reaction scheme for the inhibition of hTREK1 by lidocaine, T, hTREK1; k_i, transition rate constants; T.L, single lidocaine molecule bound to hTREK1; T.L.L*, complex of two lidocaine bound to hTREK1; $[T\text{-}L]_i$, partial inhibitory complex with single lidocaine molecule bound to one of the CTDs; and $[T\text{-}L]_i'$ or $[T\text{-}L^*]_i'$, lidocaine bound hTREK1 complete and stable inhibitory complex.

Acknowledgments

We are grateful to Prof. Steve A. N. Goldstein for providing the clone and the S348A mutant of hTREK1 and Prof. Bert Vogelstein for the AdEasy-1 system. We also thank S. Chatterjee for help in some of the molecular biology experiments.

References

Ahern CA, Eastwood AL, Dougherty DA, and Horn R (2008) Electrostatic contributions of aromatic residues in the local anesthetic receptor of voltage-gated sodium channels. *Circ Res* **102:**86–94.

Azurmendi HF, Miller SG, Whitman CP, and Mildvan AS (2005) Half-of-the-sites binding of reactive intermediates and their analogues to 4-oxalocrotonate tautomerase and induced structural asymmetry of the enzyme. *Biochemistry* **44:** 7725–7737.

Bang H, Kim Y, and Kim D (2000) TREK-2, a new member of the mechanosensitive tandem pore K^+ channel family. *J Biol Chem* **275:**17412–17419.

Ben-Abu Y, Zhou Y, Zilberberg N, and Yifrach O (2009) Inverse coupling in leak and voltage-activated K^+ channel gates underlies distinct roles in electrical signaling. *Nat Struct Mol Biol* **16:**71–79.

Benkwitz C, Garrison JC, Linden J, Durieux ME, and Hollmann MW (2003) Lidocaine enhances $G_{\alpha i}$ protein function. *Anesthesiology* **99:**1093–1101.

Bockenhauer D, Zilberberg N, and Goldstein SA (2001) KCNK2: reversible conversion of a hippocampal potassium leak into a voltage-dependent channel. *Nat Neurosci* **4:**486–491.

Carmeliet E, Morad M, Van der Heyden G, and Vereecke J (1986) Electrophysiological effects of tetracaine in single guinea-pig ventricular myocytes. *J Physiol* **376:**143–161.

Colquhoun D and Sigworth FJ (1983) Fitting and statistical analysis of single-channel records, in *Single-Channel Recording* (Sackmann B and Neher E eds) pp 191–264, Plenum Press, New York.

Cuevas J and Adams DJ (1994) Local anaesthetic blockade of neuronal nicotinic ACh receptor-channels in rat parasympathetic ganglion cells. *Br J Pharmacol* **111:**663–672.

Czirják G and Enyedi P (2002) Formation of functional heterodimers between the TASK-1 and TASK-3 two-pore domain potassium channel subunits. *J Biol Chem* **277:**5426–5432.

DeToledo JC (2000) Lidocaine and seizures. *Ther Drug Monit* **22:**320–322.

Drachman D and Strichartz G (1991) Potassium channel blockers potentiate impulse inhibition by local anesthetics. *Anesthesiology* **75:**1051–1061.

Fersht AR (1975) Demonstration of two active sites on a monomeric aminoacyl-tRNA synthetase. Possible roles of negative cooperativity and half-of-the-sites reactivity in oligomeric enzymes. *Biochemistry* **14:**5–12.

González T, Longobardo M, Caballero R, Delpón E, Tamargo J, and Valenzuela C (2001) Effects of bupivacaine and a novel local anesthetic, IQB-9302, on human cardiac K^+ channels. *J Pharmacol Exp Ther* **296:**573–583.

Hamill OP, Marty A, Neher E, Sakmann B, and Sigworth FJ (1981) Improved patch-clamp techniques for high-resolution current recording from cells and cell-free membrane patches. *Pflugers Arch* **391:**85–100.

Harinath S and Sikdar SK (2004) Trichloroethanol enhances the activity of recombinant human TREK-1 and TRAAK channels. *Neuropharmacology* **46:**750–760.

He TC, Zhou S, da Costa LT, Yu J, Kinzler KW, and Vogelstein B (1998) A simplified system for generating recombinant adenoviruses. *Proc Natl Acad Sci U S A* **95:** 2509–2514.

Hehl S and Neumcke B (1993) Negative cooperativity may explain flat concentration-response curves of ATP-sensitive potassium channels. *Eur Biophys J* **22:**1–4.

Honoré E (2007) The neuronal background K_{2P} channels: focus on TREK1. *Nat Rev Neurosci* **8:**251–261.

Johnson ME, Uhl CB, Spittler KH, Wang H, and Gores GJ (2004) Mitochondrial injury and caspase activation by the local anesthetic lidocaine. *Anesthesiology* **101:**1184–1194.

Kennard LE, Chumbley JR, Ranatunga KM, Armstrong SJ, Veale EL, and Mathie A (2005) Inhibition of the human two-pore domain potassium channel, TREK-1, by fluoxetine and its metabolite norfluoxetine. *Br J Pharmacol* **144:**821–829.

Kindler CH and Yost CS (2005) Two-pore domain potassium channels: new sites of local anesthetic action and toxicity. *Reg Anesth Pain Med* **30:**260–274.

Kindler CH, Paul M, Zou H, Liu C, Winegar BD, Gray AT, and Yost CS (2003) Amide

local anesthetics potently inhibit the human tandem pore domain background K^+ channel TASK-2 (KCNK5). *J Pharmacol Exp Ther* **306:**84–92.
Komai H and McDowell TS (2001) Local anesthetic inhibition of voltage-activated potassium currents in rat dorsal root ganglion neurons. *Anesthesiology* **94:**1089–1095.
Lesage F, Guillemare E, Fink M, Duprat F, Lazdunski M, Romey G, and Barhanin J (1996) TWIK-1, a ubiquitous human weakly inward rectifying K^+ channel with a novel structure. *EMBO J* **15:**1004–1011.
Lin X and Veenstra RD (2007) Effect of transjunctional KCl gradients on the spermine inhibition of connexin40 gap junctions. *Biophys J* **93:**483–495.
Maingret F, Honoré E, Lazdunski M, and Patel AJ (2002) Molecular basis of the voltage-dependent gating of TREK-1, a mechano-sensitive K(+) channel. *Biochem Biophys Res Commun* **292:**339–346.
Maingret F, Patel AJ, Lesage F, Lazdunski M, and Honoré E (1999) Mechano- or acid stimulation, two interactive modes of activation of the TREK-1 potassium channel. *J Biol Chem* **274:**26691–26696.
Murbartián J, Lei Q, Sando JJ, and Bayliss DA (2005) Sequential phosphorylation mediates receptor- and kinase-induced inhibition of TREK-1 background potassium channels. *J Biol Chem* **280:**30175–30184.
Nau C and Wang GK (2004) Interactions of local anesthetics with voltage-gated Na^+ channels. *J Membr Biol* **201:**1–8.
Ness TJ (2000) Intravenous lidocaine inhibits visceral nociceptive reflexes and spinal neurons in the rat. *Anesthesiology* **92:**1685–1691.
Nishizawa N, Shirasaki T, Nakao S, Matsuda H, and Shingu K (2002) The inhibition of the *N*-methyl-D-aspartate receptor channel by local anesthetics in mouse CA1 pyramidal neurons. *Anesth Analg* **94:**325–330, table of contents.
Patel AJ, Honoré E, Lesage F, Fink M, Romey G, and Lazdunski M (1999) Inhalational anesthetics activate two-pore-domain background K^+ channels. *Nat Neurosci* **2:**422–426.
Punke MA, Licher T, Pongs O, and Friederich P (2003) Inhibition of human TREK1 channels by bupivacaine. *Anesth Analg* **96:**1665–1673, table of contents.
Ragsdale DS, McPhee JC, Scheuer T, and Catterall WA (1994) Molecular determinants of state-dependent block of Na^+ channels by local anesthetics. *Science* **265:**1724–1728.
Simkin D, Cavanaugh EJ, and Kim D (2008) Control of the single channel conductance of K2P10.1 (TREK-2) by the amino-terminus: role of alternative translation initiation. *J Physiol* **586:**5651–5663.
Suzuki Y, Moriyoshi E, Tsuchiya D, and Jingami H (2004) Negative cooperativity of glutamate binding in the dimeric metabotropic glutamate receptor subtype 1. *J Biol Chem* **279:**35526–35534.
Thomas D, Plant LD, Wilkens CM, McCrossan ZA, and Goldstein SA (2008) Alternative translation initiation in rat brain yields K2P2.1 potassium channels permeable to sodium. *Neuron* **58:**859–870.
Wang R and Wu L (1997) The chemical modification of K_{Ca} channels by carbon monoxide in vascular smooth muscle cells. *J Biol Chem* **272:**8222–8226.
Zilberberg N, Ilan N, and Goldstein SA (2001) KCNKØ: opening and closing the 2-P-domain potassium leak channel entails "C-type" gating of the outer pore. *Neuron* **32:**635–648.
Zhou W, Arrabit C, Choe S, and Slesinger PA (2001) Mechanism underlying bupivacaine inhibition of G protein-gated inwardly rectifying K^+ channels. *Proc Natl Acad Sci U S A* **98:**6482–6487.

Address correspondence to: Dr. Sujit K. Sikdar, Molecular Biophysics Unit, Indian Institute of Science, Bangalore 560012, Karnataka, India. E-mail: sks@mbu.iisc.ernet.in